



OPEN

Cigarette smoking and disproportionate changes of thoracic skeletal muscles in low-dose chest computed tomography

Woo Hyeon Lim¹, Suhyun Jeong² & Chang Min Park^{1,3,4,5}✉

Association between smoking intensity and the quantity and quality of thoracic skeletal muscles (TSMs) remains unexplored. Skeletal muscle index (SMI; skeletal muscle area/height²) and percentage of normal attenuation muscle area (NAMA%) were measured to represent the quantity and quality of the skeletal muscles, respectively, and quantification was performed in pectoralis muscle at aortic arch (AA-PM), TSM at carina (C-TSM), erector spinae muscle at T12 (T12-ESM), and skeletal muscle at L1 (L1-SM). Among the 258 men (median age, 62 years [IQR: 58–69]), 183 were current smokers (median smoking intensity, 40 pack-years [IQR: 30–46]). SMI and NAMA% of AA-PM significantly decreased with pack-year ($\beta = -0.028$ and -0.076 ; $P < 0.001$ and $P = 0.021$, respectively). Smoking intensity was inversely associated with NAMA% of C-TSM ($\beta = -0.063$; $P = 0.001$), whereas smoking intensity showed a borderline association with SMI of C-TSM ($\beta = -0.023$; $P = 0.057$). Smoking intensity was associated with the change in NAMA% of L1-SM ($\beta = -0.040$; $P = 0.027$), but was not associated with SMI of L1-SM ($P > 0.05$). Neither NAMA% nor SMI of T12-ESM was affected by smoking intensity ($P > 0.05$). In conclusion, smoking intensity was associated with the change of TSMs. Its association varied according to the location of TSMs, with the most associated parts being the upper (AA-PM) and middle TSMs (C-TSM).

Efforts have been made to measure skeletal muscle areas using chest computed tomography (CT) and integrate this information into patient care^{1–9}. For example, the utilization of skeletal muscle areas as prognostic factors in patients with lung cancer or chronic obstructive pulmonary disease (COPD) has been explored^{2,3}. In addition, functional and physiologic statuses, such as forced vital capacity and 6-min walk distance, are indirectly inferred using thoracic skeletal muscle (TSM) areas^{3–5}.

Recently, a dose-dependent relationship between smoking and the lower TSM area at the carina to the skeletal muscle area at the first lumbar vertebra ratio has been reported¹⁰, suggesting that smoking be associated with disproportionate wasting of the TSM. Smoking can induce skeletal muscle dysfunction by accelerating proteolysis and inhibiting protein synthesis¹¹, which cannot explain how smoking is associated with disproportionate TSM wasting.

In addition, previous studies have simply focused on the quantity change of TSMs according to the smoking history^{10,12,13}, but both the quantity and quality of the TSM should be investigated to understand smoking-associated TSM changes. Since COPD can induce skeletal muscle dysfunction by intrinsic mechanism (at the molecular or cellular levels), extrinsic mechanism (i.e. chest wall remodeling), and mixed mechanisms (i.e. interdependence of locomotor and ventilatory muscles)^{14,15}, COPD should be considered as an important mediator between smoking and disproportionate TSM wasting.

¹Department of Radiology, Seoul National University Hospital, 101 Daehak-ro, Jongno-gu, Seoul 03080, Republic of Korea. ²Department of Radiology, Namwon Medical Center, 365 Chungjeong-no, Namwon, Jeollabuk-do 55726, Republic of Korea. ³Department of Radiology, Seoul National University College of Medicine, 101 Daehak-ro, Jongno-gu, Seoul 03080, Republic of Korea. ⁴Institute of Radiation Medicine, Seoul National University Medical Research Center, Seoul, Republic of Korea. ⁵Institute of Medical and Biological Engineering, Medical Research Center, Seoul National University, Seoul, Republic of Korea. ✉email: cmpark.morphius@gmail.com

For the analysis of patients with COPD, a commonly used method is to adjust for the results of the pulmonary function test (PFT), including forced expiratory volume in 1 s¹³. However, PFT is not a routine practice in medical check-ups or lung cancer screening and is known to be less sensitive in the early stages of COPD¹⁶. Conversely, morphologic changes associated with COPD, such as centrilobular emphysema, total lung capacity (TLC), or bronchial wall thickening, can be easily identified using chest CT^{17,18}.

Thus, this study aimed to investigate the association between smoking intensity and the quantity and quality of the TSM after adjusting for COPD-associated changes on low-dose chest CT.

Results

Among the 258 men (median age, 62 years, [interquartile range (IQR): 58–69]) who were finally included, 183 were current smokers (median age, 61 years [IQR: 58–66]; median smoking intensity, 40 PY [IQR: 30–46]), whereas 75 were non-smokers (median age, 68 years [IQR: 62–71]) (Fig. 1). According to the smoking intensity (non-smoker vs. smokers with PY < 40 vs. smokers with PY ≥ 40), age, body-mass index (BMI), PY, skeletal muscle index (SMI) at the first lumbar vertebra (L1-SMI), percentage of normal attenuation skeletal muscle area (NAMA%) at the first lumbar vertebra (L1-SNAMA%), thoracic skeletal muscle index at the carina (C-TSMI), percentage of normal attenuation thoracic skeletal muscle area at the carina (C-TSNAMA%), pectoralis muscle index at the aortic arch (AA-PMI), square root of the wall area at internal perimeter 10 (SRWA-PI10), visual emphysema grade (VEG), and TLC were significantly different ($P < 0.05$), whereas percentage of normal attenuation pectoralis muscle area at the aortic arch (AA-PNAMA%), erector spinae muscle index at the 12th thoracic vertebra (T12-ESMI), and percentage of normal attenuation erector spinae muscle area at the 12th thoracic vertebra (T12-ESNAMA%) were comparable between the three groups ($P > 0.05$) (Table 1).

The agreement for VEG was almost perfect between the two readers ($\kappa = 0.88$). Low attenuation area less than –950 HU (LAA%950) and HU at 15th percentile (HU15%) are plotted according to VEG in Supplementary Fig. 1.

Smoking intensity and SM quantity

The distribution of SMI for every 10 PY is presented in Fig. 2. The SMI tended to decrease with increasing PY.

Smoking intensity was inversely associated with AA-PMI in all the models (β , –0.034 to –0.027; $P < 0.001$); the coefficient of PY in Model 7 was –0.028 (95% confidence interval [CI]: –0.044, –0.013; $P < 0.001$). Similarly, smoking intensity showed a significant or borderline association with C-TSMI (β , –0.036 to –0.023; $P < 0.001$ to 0.057); the association between smoking intensity and C-TSMI tended to be attenuated more significantly when VEG was included in the model (Model 7, $\beta = -0.023$; 95% CI: –0.047, 0.001; $P = 0.057$). In contrast, smoking intensity was not associated with T12-ESMI or L1-SMI ($P > 0.05$) (Table 2, Supplementary Table 1).

As a result, smoking intensity was also associated with disproportionate TSM (at the carina level) and pectoralis muscle (at the aortic arch level) wasting: C-TSMI to L1-SMI ratio (Model 7, $\beta = -0.054$; 95% CI: –0.107, –0.002; $P = 0.042$) and AA-PMI to L1-SMI ratio (Model 7, $\beta = -0.061$; 95% CI: –0.094, –0.029; $P < 0.001$) significantly decreased with PY. However, the T12-ESMI to L1-SMI ratio was not related to smoking intensity ($P = 0.535$) (Fig. 3, Supplementary Table 2).

Smoking intensity was as important a factor as COPD-associated CT findings for the quantity of the TSM at the carina (variable importance score: PY, 1.91; severe centrilobular emphysema, 1.95; TLC, 1.32; and age, 3.15) and pectoralis muscle at the aortic arch (PY, 3.59; severe centrilobular emphysema, 1.07; TLC, 1.41; and age, 0.37) (Supplementary Fig. 2).

Smoking intensity and SM quality

The distribution of NAMA% for every 10 PY is presented in Fig. 2. The NAMA% tended to decrease with increasing PY.

Smoking intensity was associated with C-TSNAMA% and AA-PNAMA% in all models (β , –0.078 to –0.063 and –0.079 to –0.074; $P < 0.001$ to 0.001 and $P = 0.008$ to 0.021, respectively). For C-TSNAMA% and AA-PNAMA%, coefficients of PY in Model 7 were –0.063 (95% CI: –0.101, –0.025; $P = 0.001$) and –0.076 (95% CI: –0.141, –0.011; $P = 0.021$), respectively. In addition, smoking intensity was an associated factor for L1-SNAMA% (Model 7, $\beta = -0.040$; 95% CI: –0.076, –0.005; $P = 0.027$). However, smoking intensity was not associated with T12-ESNAMA% (Model 7, $P = 0.643$) (Table 3, Supplementary Table 3).

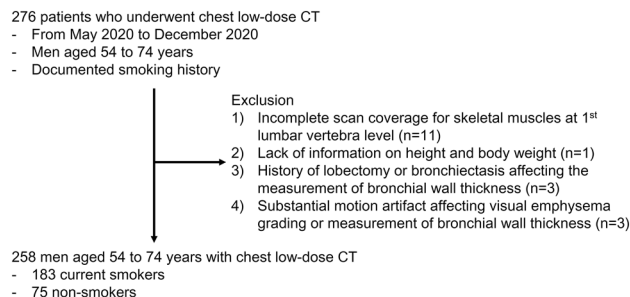


Figure 1. Study flow diagram.

Variables*	Non-smoker (n = 75)	Smokers with pack-year < 40 (n = 73)	Smokers with pack-year ≥ 40 (n = 110)	P-values
Age (years)	68 [62, 71]	58 [56, 62]	63.5 [60, 68]	< 0.001
Body weight (kg)	68.1 [62.0, 74.0]	69.1 [64.0, 73.5]	67.0 [60.0, 72.4]	0.225
Height (cm)	165.1 ± 6.7	167.5 ± 6.4	166.2 ± 6.6	0.081
Body-mass index (kg/m ²)	24.4 [23.3, 26.8]	24.7 [23.1, 26.1]	23.9 [22.6, 25.6]	0.048
Pack-year	0 [0, 0]	30 [30, 30]	45 [40, 50]	< 0.001
Skeletal muscles				
L1-SMI (cm ² /m ²)	46.3 [42.6, 49.9]	46.3 [41.7, 49.7]	43.5 [39.6, 47.4]	0.015
L1-SNAMA% (%)	62.2 [57.0, 67.1]	64.2 [58.4, 67.3]	60.5 [56.3, 64.8]	0.016
C-TSMI (cm ² /m ²)	39.1 ± 5.1	38.1 ± 5.0	36.2 ± 5.3	0.001
C-TSNAMA% (%)	62.0 [58.8, 66.5]	61.8 [56.4, 66.6]	59.8 [55.9, 64.1]	0.037
AA-PMI (cm ² /m ²)	15.4 [13.7, 17.2]	13.8 [12.7, 15.6]	13.2 [11.5, 15.2]	< 0.001
AA-PNAMA% (%)	73.8 [65.3, 78.1]	74.5 [64.6, 79.3]	70.3 [62.3, 76.9]	0.177
T12-ESMI (cm ² /m ²)	14.9 ± 3.1	14.9 ± 2.3	14.2 ± 2.7	0.103
T12-ESNAMA% (%)	71.3 [67.1, 76.2]	70.8 [64.0, 75.7]	68.3 [63.0, 73.7]	0.070
SRWA-PI10	5.39 [5.26, 5.49]	5.28 [5.15, 5.38]	5.34 [5.22, 5.51]	0.003
VEG				< 0.001
None	64 (85.3%)	51 (69.9%)	52 (47.3%)	
Trace	3 (4.0%)	6 (8.2%)	20 (18.2%)	
Mild	5 (6.7%)	9 (12.3%)	17 (15.5%)	
Moderate	3 (4.0%)	7 (9.6%)	9 (8.2%)	
Severe	0 (0.0%)	0 (0.0%)	12 (10.9%)	
LAA%950	9.8 [7.2, 13.0]	11.5 [9.4, 14.6]	12.5 [8.7, 18.0]	0.002
HU15%	-933 [-945, -921]	-941 [-950, -932]	-943 [-957, -929]	0.002
Total lung capacity (L)	4.6 ± 0.8	5.5 ± 0.9	5.5 ± 0.9	< 0.001

Table 1. Comparison of characteristics and CT-based morphologic changes according to smoking intensity. *Numerical variables with normal distribution were provided with mean ± standard deviation, while those not showing normal distribution were provided with median [interquartile range]. L1-SMI, skeletal muscle index at the first lumbar vertebra; L1-SNAMA%, percentage of normal attenuation skeletal muscle area at the first lumbar vertebra; C-TSMI, thoracic skeletal muscle index at the carina; C-TSNAMA%, percentage of normal attenuation thoracic skeletal muscle area at the carina; AA-PMI, pectoralis muscle index at the aortic arch; AA-PNAMA%, normal attenuation pectoralis muscle area at the aortic arch; T12-ESMI, erector spinae muscle index at the 12th thoracic vertebra; T12-ESNAMA%, percentage of normal attenuation erector spinae muscle area at the 12th thoracic vertebra; SRWA-PI10, square root of the wall area at internal perimeter 10; VEG, visual emphysema grade; LAA%950, low attenuation area less than -950 Hounsfield unit; HU15%, Hounsfield unit at 15th percentile.

Smoking intensity was more important than COPD-associated CT findings for C-TSNAMA% (variable importance score: PY, 3.30; severe centrilobular emphysema, 2.74; TLC, 1.57; and age, 4.87) and AA-PNAMA% (PY, 2.32; severe centrilobular emphysema, 1.32; TLC, 0.19; and age, 1.49) (Supplementary Fig. 2).

Representative cases of TSM changes in smokers and non-smokers are presented in Figs. 4 and 5, respectively.

Discussion

This study demonstrated that the relationship between smoking intensity and the changes of skeletal muscle on low-dose chest CT varied by anatomic locations, and the quantity and quality of TSMs were generally associated with smoking intensity. However, the association between change of erector spinae muscle at the 12th thoracic vertebra level and smoking intensity was not evident. In addition, the quality of skeletal muscle at the first lumbar vertebra level as defined by CT was inversely associated with PY, but the quantity did not change with smoking intensity.

Diaz et al.¹³ reported that the pectoralis muscle area and index at the aortic arch level were independent prognostic factors in smokers without airflow limitation from COPD Gene cohorts, whereas the erector spinae muscle was not prognostic. In a previous study¹², baseline lean body mass was comparable between individuals with airflow limitation and current smokers without evidence of airflow limitation in men aged 70–79 years. In these studies^{12, 13}, the relationship between smoking intensity and TSM changes was not comprehensively investigated. Lim et al.¹⁰ reported a dose-dependent disproportionate decrease in TSM at the carina level according to PY; however, other parts of the TSMs were not investigated, and COPD-associated CT findings were not considered, which might be the most important mediator between smoking and TSM wasting.

This study investigated the relationship between smoking intensity and TSM changes in various body parts in terms of muscle quantity and quality, after adjusting for several important confounders or mediators, such as age, BMI, and COPD-associated CT findings. Interestingly, the association between the smoking intensity

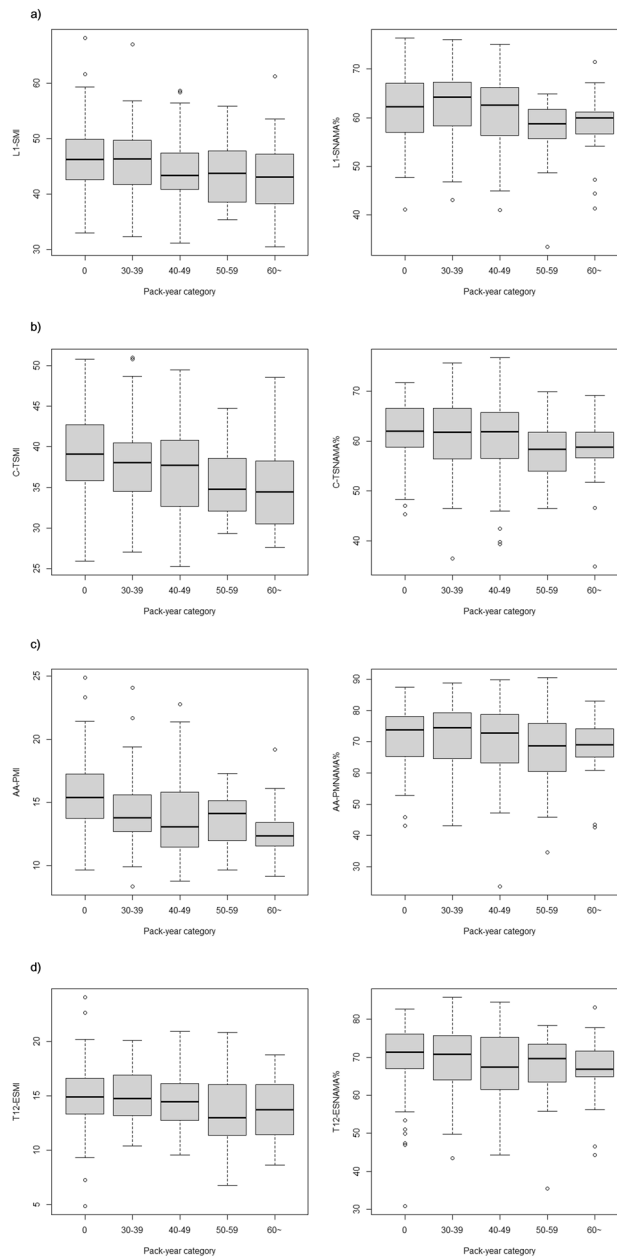


Figure 2. The quantity and quality of skeletal muscles according to smoking intensity: **(a)** skeletal muscle at the first lumbar vertebra level (L1-SMI, skeletal muscle index at the first lumbar vertebra; L1-SNAMA%, percentage of normal attenuation skeletal muscle area at the first lumbar vertebra), **(b)** thoracic skeletal muscle at the carina level (C-TSMI, thoracic skeletal muscle index at the carina; C-TSNAMA%, percentage of normal attenuation thoracic skeletal muscle area at the carina), **(c)** pectoralis muscle at the aortic arch level (AA-PMI, pectoralis muscle index at the aortic arch; AA-PNAMA%, normal attenuation pectoralis muscle area at the aortic arch), and **(d)** erector spinae muscle at the 12th thoracic vertebra level (T12-ESMI, erector spinae muscle index at the 12th thoracic vertebra; T12-ESNAMA%, percentage of normal attenuation erector spinae muscle area at the 12th thoracic vertebra).

and TSMs seemed to vary according to the anatomical location of the TSMs, which may be related to their role in respiration. Because the external intercostal, pectoralis, trapezius, and serratus anterior muscles are the assessed parts of the TSMs at the carina level, TSMs at this level might serve as inspiratory accessory muscles^{19,20}. Conversely, skeletal muscles at the first lumbar vertebra level partly contribute to either respiration (i.e., accessory expiratory muscles: anterolateral abdominal wall muscles) or work against gravitation (i.e., antigravity muscles: erector spinae muscles)^{3,21}. Our results might suggest that the greater the degree of involvement in respiration, the greater the effect of smoking intensity on TSM quantification. These results might also suggest that the subclinical work of breathing exist in heavy smokers, which is not fully captured on the PFT¹⁶.

Model	C-TSMI	P-values	AA-PMI	P-values	T12-ESMI	P-value	L1-SMI*	P-value
Model 1	-0.028 (-0.051, -0.006)	0.013	-0.031 (-0.046, -0.017)	<0.001	0.000 (-0.011, 0.011)	0.981	-0.018 (-0.048, 0.012)	0.239
Model 2	-0.030 (-0.052, -0.007)	0.009	-0.028 (-0.043, -0.014)	<0.001	-0.003 (-0.014, 0.008)	0.625	-0.024 (-0.054, 0.006)	0.110
Model 3	-0.036 (-0.057, -0.015)	<0.001	-0.034 (-0.047, -0.020)	<0.001	-0.003 (-0.013, 0.008)	0.633	-0.022 (-0.050, 0.006)	0.123
Model 4	-0.023 (-0.047, 0.000)	0.050	-0.027 (-0.042, -0.011)	<0.001	-0.001 (-0.012, 0.011)	0.924	-0.020 (-0.051, 0.012)	0.215
Model 5	-0.028 (-0.051, -0.006)	0.013	-0.032 (-0.047, -0.017)	<0.001	0.000 (-0.011, 0.011)	0.963	-0.018 (-0.048, 0.012)	0.236
Model 6	-0.029 (-0.052, -0.007)	0.011	-0.030 (-0.044, -0.015)	<0.001	-0.004 (-0.015, 0.007)	0.439	-0.025 (-0.056, 0.005)	0.098
Model 7	-0.023 (-0.047, 0.001)	0.057	-0.028 (-0.044, -0.013)	<0.001	-0.002 (-0.014, 0.009)	0.693	-0.021 (-0.053, 0.011)	0.197

Table 2. Effect of pack-year of smoking on skeletal muscle quantity. All models were adjusted for age, body-mass index, skeletal muscle index at the first lumbar vertebra, and chronic obstructive pulmonary disease associated features: Model 1, visual emphysema grade (VEG) only; Model 2, total lung capacity (TLC) only; Model 3, square root of the wall area at internal perimeter of 10 mm (SRWA-PI10) only; Model 4, VEG and TLC; Model 5, VEG and SRWA-PI10; Model 6, TLC and SRWA-PI10; Model 7, VEG, TLC, and SRWA-PI10. Presented values were coefficients of pack-year with 95th percentile confidence interval in parenthesis.

*All models were adjusted for age, body-mass index, and chronic obstructive pulmonary disease associated features. C-TSMI, thoracic skeletal muscle index at the carina; T12-ESMI, erector spinae muscle index at the 12th thoracic vertebra; AA-PMI, pectoralis muscle index at the aortic arch; L1-SMI, skeletal muscle index at the first lumbar vertebra.

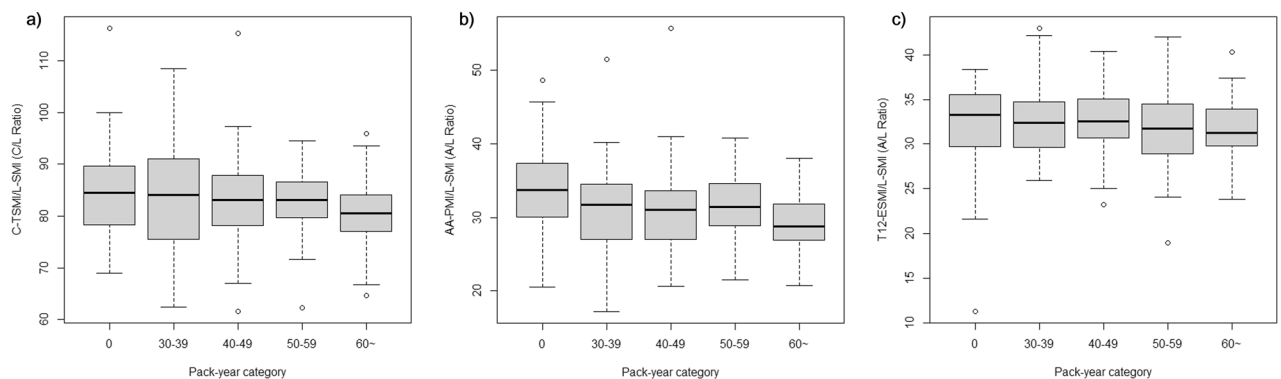


Figure 3. Disproportionate skeletal muscles wasting according to smoking intensity: (a) C/L ratio (thoracic skeletal muscle index at the carina to skeletal muscle index at the first lumbar [L1-SMI] ratio), (b) A/L ratio (pectoralis muscle index at the aortic arch to L1-SMI ratio), and (c) T/L ratio (erector spinae muscle index at the 12th thoracic vertebra to L1-SMI ratio).

On the basis of these results, the use of skeletal muscles at the first lumbar vertebra level or erector spinae muscles at the 12th thoracic vertebra level may be recommended for the quantification of skeletal muscles on low-dose chest CT, as these parts are less significantly associated with smoking. In addition, smoking intensity should always be considered when assessing the TSM at the carina and pectoralis muscle at the aortic arch levels^{4, 3-5, 7, 22, 23}, because smoking intensity is as important as COPD-associated CT findings in the quantification of these TSMs.

The association between the smoking intensity and TSM change was attenuated when VEG was included in the model, whereas the attenuation was less significant after adjusting for bronchial wall thickness. These findings were consistent with those of previous studies that showed that skeletal muscle wasting was more common in emphysema-predominant COPD than in chronic bronchitis^{4, 22}. Since the structural pattern of the airway is substantially different between sexes²⁴, these results need to be validated in women.

This study had some limitations. As this was a retrospective study, an unidentified bias could exist. For example, PY were a self-reported measure that was vulnerable to variability. Because PY based on medical records tend to be under-reported²⁵, the association between smoking and TSM changes might be accentuated. In addition, the influence of underlying diseases could not be identified in this study population because this information was absent in some individuals. However, the presence of hypertension, diabetes, and dyslipidemia did not show a significant effect on sarcopenia in a previous study¹⁰. Thus, a focused evaluation of the association between TSM changes, smoking, and COPD-associated CT findings was considered acceptable. Recently, history of severe acute respiratory syndrome coronavirus-2 disease (COVID-19) has emerged as a novel cause of skeletal

Model	C-TSNAMA%	P-value	AA-PNAMA%	P-value	T12-ESNAMA%	P-value	L1-SNAMA%	P-value
Model 1	-0.073 (-0.108, -0.037) ^a	<0.001	-0.074 (-0.135, -0.014)	0.016	-0.033 (-0.082, 0.016)	0.188	-0.041 (-0.075, -0.008)	0.015
Model 2	-0.065 (-0.100, -0.029)	<0.001	-0.079 (-0.140, -0.018)	0.011	-0.027 (-0.076, 0.023)	0.296	-0.045 (-0.079, -0.012)	0.009
Model 3	-0.078 (-0.112, -0.044)	<0.001	-0.078 (-0.136, -0.021)	0.008	-0.051 (-0.099, -0.004)	0.034	-0.051 (-0.083, -0.020)	0.002
Model 4	-0.063 (-0.100, -0.025)	0.001	-0.077 (-0.141, -0.013)	0.018	-0.012 (-0.063, 0.039)	0.640	-0.038 (-0.073, -0.003)	0.034
Model 5	-0.073 (-0.109, -0.038)	<0.001	-0.074 (-0.135, -0.013)	0.017	-0.034 (-0.083, 0.015)	0.177	-0.042 (-0.075, -0.009)	0.014
Model 6	-0.065 (-0.101, -0.029)	<0.001	-0.078 (-0.139, -0.016)	0.014	-0.027 (-0.077, 0.024)	0.300	-0.047 (-0.081, -0.013)	0.007
Model 7	-0.063 (-0.101, -0.025)	0.001	-0.076 (-0.141, -0.011)	0.021	-0.012 (-0.064, 0.040)	0.643	-0.040 (-0.076, -0.005)	0.027

Table 3. Effect of pack-year of smoking on skeletal muscle quality. All models were adjusted for age, body-mass index, skeletal muscle index at the first lumbar vertebra, and chronic obstructive pulmonary disease associated features: Model 1, visual emphysema grade (VEG) only; Model 2, total lung capacity (TLC) only; Model 3, square root of the wall area at internal perimeter of 10 mm (SRWA-PI10) only; Model 4, VEG and TLC; Model 5, VEG and SRWA-PI10; Model 6, TLC and SRWA-PI10; Model 7, VEG, TLC, and SRWA-PI10. Presented values were coefficients of pack-year with 95th percentile confidence interval in parenthesis. C-TSNAMA%, percentage of normal attenuation thoracic skeletal muscle area at the carina; AA-PNAMA%, normal attenuation pectoralis muscle area at the aortic arch; T12-ESNAMA%, percentage of normal attenuation erector spinae muscle area at the 12th thoracic vertebra; L1-SNAMA%, percentage of normal attenuation skeletal muscle area at the first lumbar vertebra.

muscle changes²⁶. As the prevalence of severe COVID-19 was extremely low in our country during the study period²⁷, it could be assumed that the impact of COVID-19 on the results of this study seemed to be minimal. As current female smokers are rare and the skeletal muscles of women are significantly smaller than those of men, this study only included men. Although appropriate validation is required in women, we expect that differences due to sex may not be significant. While this study provided a consistent association between smoking intensity and disproportionate TSM wasting in a temporally different dataset from that of a previous study¹⁰, the clinical importance of disproportionate TSM wasting needs to be explored in future studies. It is also needed to evaluate whether disproportionate TSM wasting is observed in heavy smokers aged over 74 years. As systemic inflammation could also contribute to the skeletal muscle wasting in smokers, it might be important to assess the level of systemic inflammatory markers¹¹. Finally, although a substantial number of current smokers could exhibit COPD-associated CT abnormalities without airflow limitation²⁸, COPD-associated CT findings were adjusted as a possible mediator between smoking and TSM wasting rather than PFT results. Thus, evaluation after adjusting for PFT results and systemic inflammatory markers might provide comprehensive understanding for the relationship between smoking, airflow limitation, systemic inflammation and TSM changes^{11,29}, and our results need to be validated under such study design.

In conclusion, the association between smoking intensity and TSM changes in terms of quantity and quality varied according to the location of the TSMs. Thus, quantification of skeletal muscles at the lower thoracic or upper lumbar level may be recommended to explore the clinical importance in patient care using chest CT. Smoking intensity should be considered when the upper or middle TSMs are used for quantification. The clinical importance of disproportionate TSM wasting in heavy smokers should be explored in future studies.

Materials and methods

This retrospective study was approved by Public Institutional Review Board designated by Ministry of Health and Welfare, Republic of Korea (approval number: P01-202102-21-011) with a waiver of informed consent. All studies were performed in accordance with relevant guidelines and regulations.

Patients

Between May and December 2020, consecutive patients who underwent low-dose chest CT without intravenous contrast medium administration at the Namwon Medical Center were retrospectively recruited for this study. These patients comprised those who underwent low-dose chest CT as part of a national lung cancer screening program in the Republic of Korea³⁰ or their medical check-ups^{31,32}.

The inclusion criteria were as follows: 1) men aged 54–74 years and 2) a documented history of smoking. Patients were excluded from this study for the following reasons: 1) incomplete scan coverage of skeletal muscles at the first lumbar vertebra (n = 11); 2) lack of information on height and body weight (n = 1); 3) history of lobectomy or bronchiectasis that could affect bronchial wall thickness measurement (n = 3); and 4) substantial motion artifacts affecting VEG or bronchial wall thickness measurement (n = 3; Fig. 1).

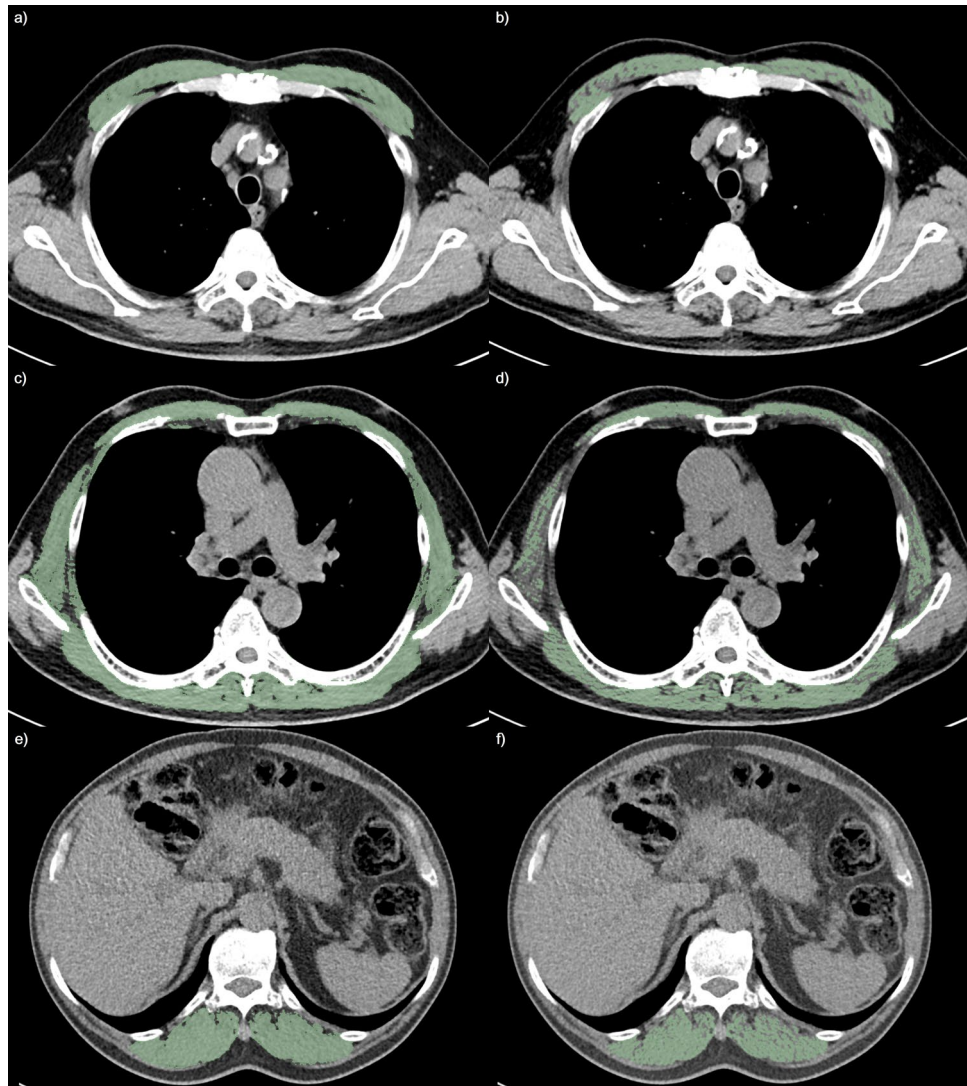


Figure 4. Thoracic skeletal muscle change in a current smoker: In a 68 year-old current smoker with 40 pack-year (body weight 58.2 kg, height 157.4 cm, body-mass index 23.5 kg/m²) showed severe degree of centrilobular emphysema, total lung capacity of 4.3L, and 5.22 mm of the square root of the wall area at internal perimeter of 10 mm: (a,b) pectoralis muscle index at the aortic arch (AA-PMI) and percentage of normal attenuation pectoralis muscle area at the aortic arch (AA-PNAMA%) were 10.7cm²/m² and 61.4%, respectively; (c,d) thoracic skeletal muscle index at the carina (C-TSMI) and percentage of normal attenuation thoracic skeletal muscle area at the carina (C-TSNAMA%) were 34.4cm²/m² and 47.6%, respectively; and (e,f) erector spinae muscle index at the 12th thoracic vertebra (T12-ESMI) and percentage of normal attenuation erector spinae muscle area at the 12th thoracic vertebra (T12-ESNAMA%) were 13.9cm²/m² and 65.8%, respectively. The SMI at the first lumbar vertebra (L1-SMI) and percentage of normal attenuation skeletal muscle area at the first lumbar vertebra (L1-SNAMA%) were 42.1cm²/m² and 53.5%, respectively (not presented).

CT imaging protocols

CT imaging was performed using SOMATOM Definition AS+ (Siemens) at 50 mAs/100 kVp. The CT images were reconstructed using three methods: 1) axial images with a 1.0-mm slice thickness and I50f. filter, 2) axial images with a 2.5-mm slice thickness and I30f. filter, and 3) coronal images with a 2.5-mm slice thickness and I50f. filter.

SM segmentation

With axial images of 2.5-mm thickness, the SMAs were segmented semi-automatically using an open-source software program (3D Slicer Chest Imaging Platform, version 4.10.2) with fine manual editing by one of the authors (W.H.L.; 8 years of experience in chest imaging). HU ranging from -29 to 150 were considered skeletal muscles, and HU ranging from 30 to 150 were classified as a normal attenuation skeletal muscle area³³. For this study, skeletal muscle area at the first lumbar vertebra^{1,6,7}, erector spinae muscle area at the 12th thoracic vertebra level^{3,8,9}, thoracic skeletal muscle area at the carina level⁵, and pectoralis muscle area at the aortic arch level^{1,3,4,7}

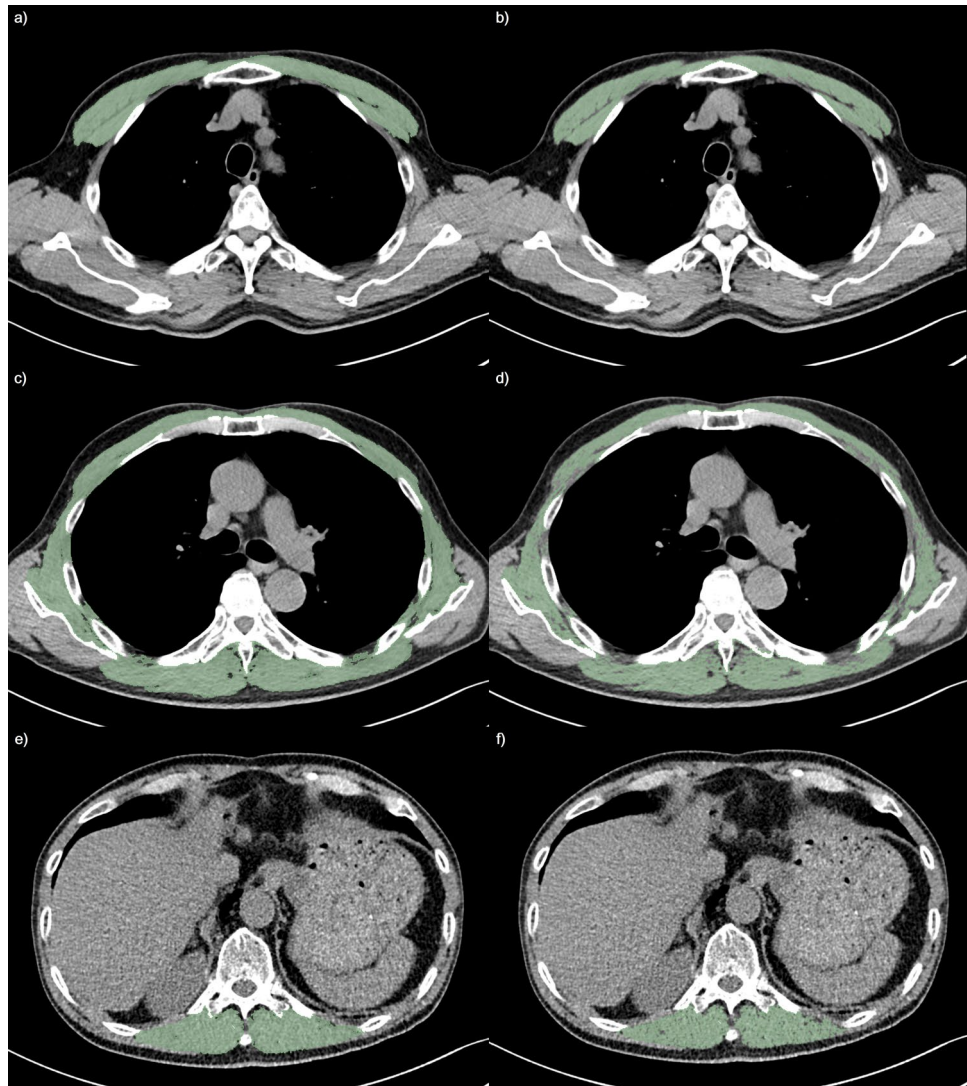


Figure 5. Thoracic skeletal muscle change in a non-smoker: In a 69 year-old men without documented smoking history (body weight 71 kg, height 172.7 cm, body-mass index 23.8 kg/m²) showed absence of centrilobular emphysema, total lung capacity of 5.2L, and 5.06 mm of square root of the wall area at internal perimeter of 10 mm: (a,b) pectoralis muscle index at the aortic arch (AA-PMI) and percentage of normal attenuation pectoralis muscle area at the aortic arch (AA-PNAMA%) were 13.9cm²/m² and 77.8%, respectively; (c,d) thoracic skeletal muscle index at the carina (C-TSMI) and percentage of normal attenuation thoracic skeletal muscle area at the carina (C-TSNAMA%) were 36.4cm²/m² and 64.7%, respectively; and (e,f) erector spinae muscle index at the 12th thoracic vertebra (T12-ESMI) and percentage of normal attenuation erector spinae muscle area at the 12th thoracic vertebra (T12-ESNAMA%) were 12.2cm²/m² and 77.6%, respectively. The SMI at the first lumbar vertebra (L1-SMI) and percentage of normal attenuation skeletal muscle area at the first lumbar vertebra (L1-SNAMA%) were 40.6cm²/m² and 68.4%, respectively (not presented).

were segmented. The AA-PMI to L1-SMI ratio, C-TSMI to L1-SMI ratio, and T12-ESMI to L1-SMI ratio were calculated¹⁰. The NAMA% (normal attenuation skeletal muscle area/total skeletal muscle area × 100) for each muscle area was calculated³⁴. The SMI (skeletal muscle area/height²) and NAMA% were representative of the quantity and quality of each skeletal muscle, respectively. The L1-SMI was representative of lean body mass on chest CT¹⁰. The pectoralis muscle at the aortic arch, TSM at the carina, and erector spinae muscle at the 12th thoracic vertebra level were representatives of the upper, middle, and lower TSMs, respectively.

COPD-associated changes

To evaluate the bronchial wall thickness, SRWA-PI10 was calculated as previously described by the author (W.H.L.)^{35,36}, with 1.0-mm-thick images using the zero-crossing method (3D Slicer). Small airways (internal perimeter < 6 mm) and airways with bronchiectasis were carefully avoided³⁵. The TLC was obtained with 1.0-mm-thick images using 3D Slicer, and the TLC was not adjusted for the height³⁷.

To evaluate the degree of centrilobular emphysema, VEG (absent, trace, mild, moderate, or severe) was independently performed by two radiologists (W.H.L. and S.J.; 30 years of experience in chest imaging)¹⁷. Patients' information on smoking PY was blinded during VEG. Confluent and advanced destructive emphysema was classified as severe¹⁷. The presence of paraseptal emphysema was not considered in this study, as the standardized visual grading system for paraseptal emphysema is lacking and the attribution of paraseptal emphysema to extrapulmonary and systemic abnormalities is less significant than that of centrilobular emphysema²⁶. The discrepancies between the two readers were resolved by consensus. As supplementary data, LAA%950 and HU15% were also calculated using 3D Slicer^{38, 39}.

Clinical information

Anthropometric data (height and body weight) and smoking status were collected from electronic medical records. The BMI (body weight/height²) was calculated using anthropometric data. The PY data collected from current smokers. Underlying medical diseases were not included in this study because such information is not routinely collected in the national lung cancer screening program.

Statistical analyses

Comparisons of numerical variables were performed using a one-way analysis of variance or the Kruskal–Wallis test, as appropriate, after evaluating the normality of the parameters. Frequencies were compared using the chi-square test.

Agreement of VEG between the two readers was evaluated using Cohen's Kappa coefficient (κ), and the κ was interpreted as follows: 1) slight agreement (κ , 0.01–0.20), 2) fair agreement (κ , 0.21–0.40), 3) moderate agreement (κ , 0.41–0.60), 4) substantial agreement (κ , 0.61–0.80), and 5) almost perfect agreement (κ , 0.81–0.99)⁴⁰.

The effects of smoking on the TSM changes were assessed after adjusting for age, BMI, L1-SMI, and COPD-associated CT changes. Seven models with combinations of VEG, TLC, and SRWA-PI10 were built to assess the effects of smoking (Model 1: VEG only; Model 2: TLC only; Model 3: SRWA-PI10 only; Model 4: VEG and TLC; Model 5: VEG and SRWA-PI10; Model 6: TLC and SRWA-PI10; and Model 7 [full model]: VEG, TLC, and SRWA-PI10). Variable importance scores were obtained for Model 7.

Statistical analyses were performed using the R (version 4.1.2). In this study, *P*-values less than 0.05 were considered statistically significant. A variance inflation factor greater than 10 indicated the presence of multicollinearity.

Data availability

The datasets generated or analyzed during the study are available from the corresponding author on reasonable request.

Received: 22 May 2023; Accepted: 31 October 2023

Published online: 17 November 2023

References

- Sanders, K. J. C., Degens, J., Dingemans, A. C. & Schols, A. Cross-sectional and longitudinal assessment of muscle from regular chest computed tomography scans: L1 and pectoralis muscle compared to L3 as reference in non-small cell lung cancer. *Int. J. Chron. Obstruct. Pulmon. Dis.* **14**, 781–789 (2019).
- Kim, E. Y. *et al.* Prognostic significance of CT-determined sarcopenia in patients with small-cell lung cancer. *J. Thorac. Oncol.* **10**, 1795–1799 (2015).
- Tanimura, K. *et al.* Quantitative assessment of erector spinae muscles in patients with chronic obstructive pulmonary disease. Novel chest computed tomography-derived index for prognosis. *Ann. Am. Thorac. Soc.* **13**, 334–341 (2016).
- McDonald, M. L. *et al.* Quantitative computed tomography measures of pectoralis muscle area and disease severity in chronic obstructive pulmonary disease. A cross-sectional study. *Ann. Am. Thorac. Soc.* **11**, 326–334 (2014).
- Rozenberg, D. *et al.* Thoracic muscle cross-sectional area is associated with hospital length of stay post lung transplantation: a retrospective cohort study. *Transpl. Int.* **30**, 713–724 (2017).
- Recio-Boiles, A. *et al.* Enhancing evaluation of sarcopenia in patients with non-small cell lung cancer (NSCLC) by assessing skeletal muscle index (SMI) at the first lumbar (L1) level on routine chest computed tomography (CT). *Support Care Cancer.* **26**, 2353–2359 (2018).
- Kim, E. Y. *et al.* Evaluation of sarcopenia in small-cell lung cancer patients by routine chest CT. *Support Care Cancer.* **24**, 4721–4726 (2016).
- Moon, S. W. *et al.* Thoracic skeletal muscle quantification: low muscle mass is related with worse prognosis in idiopathic pulmonary fibrosis patients. *Respir. Res.* **20**, 35 (2019).
- Nakano, A. *et al.* Early decrease in erector spinae muscle area and future risk of mortality in idiopathic pulmonary fibrosis. *Sci. Rep.* **10**, 2312 (2020).
- Lim, W. H. & Park, C. M. Validation for measurements of skeletal muscle areas using low-dose chest computed tomography. *Sci. Rep.* **12**, 463 (2022).
- Degens, H., Gayan-Ramirez, G. & van Hees, H. W. Smoking-induced skeletal muscle dysfunction: from evidence to mechanisms. *Am. J. Respir. Crit. Care Med.* **191**, 620–625 (2015).
- van den Borst, B. *et al.* Is age-related decline in lean mass and physical function accelerated by obstructive lung disease or smoking?. *Thorax.* **66**, 961–969 (2011).
- Diaz, A. A. *et al.* Pectoralis muscle area and mortality in smokers without airflow obstruction. *Respir. Res.* **19**, 62 (2018).
- Barnes, P. J. & Celli, B. R. Systemic manifestations and comorbidities of COPD. *Eur. Respir. J.* **33**, 1165–1185 (2009).
- Jaitovich, A. & Barreiro, E. Skeletal muscle dysfunction in chronic obstructive pulmonary disease. What we know and can do for our patients. *Am. J. Respir. Crit. Care Med.* **198**, 175–186 (2018).
- Fan, L. *et al.* Capability of differentiating smokers with normal pulmonary function from COPD patients: a comparison of CT pulmonary volume analysis and MR perfusion imaging. *Eur. Radiol.* **23**, 1234–1241 (2013).
- Lynch, D. A. *et al.* CT-definable subtypes of chronic obstructive pulmonary disease: A statement of the Fleischner society. *Radiology.* **277**, 192–205 (2015).

18. Koo, H. J. *et al.* Prediction of pulmonary function in patients with chronic obstructive pulmonary disease: Correlation with quantitative CT parameters. *Korean J. Radiol.* **20**, 683–692 (2019).
19. Kim, K. S. *et al.* Effects of breathing maneuver and sitting posture on muscle activity in inspiratory accessory muscles in patients with chronic obstructive pulmonary disease. *Multidiscip. Respir Med.* **7**, 9 (2012).
20. Trevisan, M. E. *et al.* Diaphragmatic amplitude and accessory inspiratory muscle activity in nasal and mouth-breathing adults: a cross-sectional study. *J. Electromyogr. Kinesiol.* **25**, 463–468 (2015).
21. Ratnovsky, A., Elad, D. & Halpern, P. Mechanics of respiratory muscles. *Respir. Physiol. Neurobiol.* **163**, 82–89 (2008).
22. Bak, S. H., Kwon, S. O., Han, S. S. & Kim, W. J. Computed tomography-derived area and density of pectoralis muscle associated disease severity and longitudinal changes in chronic obstructive pulmonary disease: a case control study. *Respir. Res.* **20**, 226 (2019).
23. O'Brien, M. E. *et al.* CT pectoralis muscle area is associated with DXA lean mass and correlates with emphysema progression in a tobacco-exposed cohort. *Thorax.* **78**, 394–401 (2023).
24. Bhatt, S. P. *et al.* Sex differences in airways at chest CT: Results from the COPDGene cohort. *Radiology.* **305**, 699–708 (2022).
25. Modin, H. E. *et al.* Pack-year cigarette smoking history for determination of lung cancer screening eligibility. Comparison of the electronic medical record versus a shared decision-making conversation. *Ann. Am. Thorac. Soc.* **14**, 1320–1325 (2017).
26. Soares, M. N. *et al.* Skeletal muscle alterations in patients with acute Covid-19 and post-acute sequelae of Covid-19. *J. Cachexia Sarcopenia Muscle.* **13**, 11–22 (2022).
27. https://kosis.kr/covid/covid_index.do (accessed date: 2023–09–30).
28. Maetani, T. *et al.* Centrilobular emphysema is associated with pectoralis muscle reduction in current smokers without airflow limitation. *Respiration.* **102**, 194–202 (2023).
29. Vanfleteren, L. E. G. W. *et al.* Clusters of comorbidities based on validated objective measurements and systemic inflammation in patients with chronic obstructive pulmonary disease. *Am. J. Respir. Crit. Care Med.* **187**, 728–735 (2013).
30. Kim, H. Y. National lung cancerscreening in Korea: Introduction and imaging quality control. *J. Korean Soc. Radiol.* **80**, 826–836 (2019).
31. Chang, Y. *et al.* Alcoholic and non-alcoholic fatty liver disease and associations with coronary artery calcification: Evidence from the Kangbuk Samsung Health Study. *Gut.* **68**, 1667–1675 (2019).
32. Lee, C. *et al.* Health and prevention enhancement (H-PEACE): A retrospective, population-based cohort study conducted at the Seoul National University Hospital Gangnam Center, Korea. *MJ Open.* **8**, e019327 (2018).
33. Kim, D. W. *et al.* Reliability of skeletal muscle area measurement on CT with different parameters: A phantom study. *Korean J. Radiol.* **22**, 624–633 (2021).
34. Kim, H. K. *et al.* Age-related changes in muscle quality and development of diagnostic cutoff points for myosteatosis in lumbar skeletal muscles measured by CT scan. *Clin. Nutr.* **40**, 4022–4028 (2021).
35. Grydeland, T. B. *et al.* Quantitative computed tomography: emphysema and airway wall thickness by sex, age and smoking. *Eur. Respir. J.* **34**, 858–865 (2009).
36. Patel, B. D. *et al.* Airway wall thickening and emphysema show independent familial aggregation in chronic obstructive pulmonary disease. *Am. J. Respir. Crit. Care Med.* **178**, 500–505 (2008).
37. Hackx, M. *et al.* Effect of total lung capacity, gender and height on CT airway measurements. *Br. J. Radiol.* **90**, 20160898 (2017).
38. Regan, E. A. *et al.* Genetic epidemiology of COPD (COPDGene) study design. *COPD.* **7**, 32–43 (2010).
39. Ostridge, K. & Wilkinson, T. M. Present and future utility of computed tomography scanning in the assessment and management of COPD. *Eur. Respir. J.* **48**, 216–228 (2016).
40. Viera, A. J. & Garrett, J. M. Understanding interobserver agreement: The kappa statistic. *Fam. Med.* **37**, 360–363 (2005).

Author contributions

W.H.L. contributed to conceptualization, data curation, formal analysis, investigation, methodology, visualization, writing (original draft), and writing (review & editing). S.J. contributed to data curation, and writing (review & editing). C.M.P. contributed to conceptualization, supervision, validation, and writing (review & editing).

Competing interests

The authors declare no competing interests.

Additional information

Supplementary Information The online version contains supplementary material available at <https://doi.org/10.1038/s41598-023-46360-0>.

Correspondence and requests for materials should be addressed to C.M.P.

Reprints and permissions information is available at www.nature.com/reprints.

Publisher's note Springer Nature remains neutral with regard to jurisdictional claims in published maps and institutional affiliations.



Open Access This article is licensed under a Creative Commons Attribution 4.0 International License, which permits use, sharing, adaptation, distribution and reproduction in any medium or format, as long as you give appropriate credit to the original author(s) and the source, provide a link to the Creative Commons licence, and indicate if changes were made. The images or other third party material in this article are included in the article's Creative Commons licence, unless indicated otherwise in a credit line to the material. If material is not included in the article's Creative Commons licence and your intended use is not permitted by statutory regulation or exceeds the permitted use, you will need to obtain permission directly from the copyright holder. To view a copy of this licence, visit <http://creativecommons.org/licenses/by/4.0/>.

© The Author(s) 2023